

Single Cell Analysis of Complex Thymus Stromal Cell Populations: Rapid Thymic Epithelia Preparation Characterizes Radiation Injury

Kirsten M. Williams, M.D.¹, Heather Mella, B.A.¹, Philip J. Lucas, Ph.D.¹, Joy A. Williams, Ph.D.², William Telford, Ph.D.¹, and Ronald E. Gress, M.D.¹

Abstract

Thymic epithelial cells (TECs) and dendritic cells are essential for the maintenance of thymopoiesis. Because these stromal elements define the progenitor niche, provide critical survival signals and growth factors, and direct positive and negative selection, detailed study of these populations is necessary to understand important elements for thymic renewal after cytotoxic injury. Study of TEC is currently hindered by lengthy enzymatic separation techniques with decreased viability. We present a new rapid separation technique that yields consistent viable TEC numbers in a quarter of the prior preparation time. Using this new procedure, we identify changes in stromal populations following total body irradiation (TBI). By flow cytometry, we show that TBI significantly depletes UEA+ medullary TEC, while sparing Ly51+ CD45- cells. Further characterization of the Ly51+ subset reveals enrichment of fibroblasts (CD45- Ly51+ MHCII-), while cortical TECs (CD45- Ly51+ MHCII+) were markedly reduced. Dendritic cells (CD11c+ CD45+) were also decreased following TBI. These data suggest that cytotoxic preparative regimens may impair thymic renewal by reducing critical populations of cortical and medullary TEC, and that such thymic damage can be assessed by this new rapid separation technique, thereby providing a means of assessing optimal conditioning pretransplant for enhancing thymic-dependent immune reconstitution posttransplant.

Keywords: thymic epithelial cell, separation, radiation

Introduction

Impaired thymopoiesis contributes to the immune deficiency observed following lymphopenia or allogeneic hematopoietic stem cell transplantation (HSCT).¹⁻³ The thymus is the fundamental site for *de novo* T-cell development where thymocytes, expressing a diverse repertoire of T-cell receptors, are generated. The thymus is also a major contributor to central tolerance by deleting autoreactive T cells. In the absence of thymic renewal following lymphopenia, an oligoclonal repertoire of T cells is sustained, resulting in impaired eradication of tumors and infections, and increased incidence of auto- or alloimmunity (graft-versus-host disease).³⁻⁷ Clinical data suggest that cytoreductive cancer therapies (chemotherapy and radiation) induce thymic damage, compromising immune reconstitution indefinitely after allogeneic transplantation and that minimizing this damage may preserve thymic function. Reduced-intensity transplant preparative regimens have been shown to result in greater CD4+ T-cell numbers, a more diverse T-cell repertoire, and higher peripheral T-cell receptor excision circle frequency as compared to more toxic myeloablative regimens.⁸⁻¹¹ Thus, study of the critical elements involved in thymic renewal and ways to minimize thymic injury may be of critical importance to successful immune reconstitution and patient survival following HSCT and chemotherapeutic treatment for cancer.

Emerging data suggest that thymic renewal is dependent on functional thymic epithelia. Agents that expand thymic epithelia have been shown to increase thymopoiesis, including androgen withdrawal,^{12,13} insulin-like growth factor 1 and growth hormone,^{14,15} and keratinocyte growth factor.^{16,17} Thymic epithelial cells (TECs) mediate central tolerance and support thymopoiesis. TECs produce essential growth factors (IGF-1, CXCL12),^{14,18,19} cytokines (IL-7),²⁰ and chemokines (CCR7L, CCL25).^{12,21-24} These elements enhance precursor immigration (CCL25, CCL21),^{12,24,25} induce thymocyte proliferation and survival (IL-7),^{26,27} and direct thymocyte migration and development (CCL25, CXCL12).^{12,18,22} Furthermore, data have suggested that TEC may even regulate

the thymic niche, controlling the entry of early progenitors and restricting thymopoiesis.^{12,28,29} Thus, the study of TEC subsets and their products should provide important clues regarding the mechanism of thymus involution, damage, and regeneration.

To date, the study of TEC has been hindered by laborious and time-consuming isolation techniques. Much work has been devoted to the isolation and separation of TEC for subsequent analysis.³⁰⁻³⁴ TEC purification is challenging because TECs are rare cells³⁰; TEC interdigitate³⁵ with other TEC and thymocytes and these connections are solidified by extracellular matrix and collagen³⁶; TEC viability may be quickly compromised because of the extended manipulation time needed by current separation techniques. Gray et al. developed the TEC isolation techniques commonly cited in the literature.^{30,31} This method involves agitation to remove thymocytes followed by four collagenase/dispase/DNase digestions at 37°C with frequent agitation. At the conclusion of each digestion step, undigested material remains at the bottom of the tube and the supernatant containing separated cells is removed and placed on ice. Replacement enzyme cocktail (collagenase/dispase/DNase) is then added to the remaining fragments for further digestion. While this technique successfully separates TEC, permitting phenotyping by flow cytometry analysis, the TEC and thymocyte flow cytometry profiles of each digestion fraction are markedly different.³⁰ Thus, the subtle changes in the length of exposure to the enzyme cocktail³⁰ could influence the ultimate result, resulting in variable final cell numbers and proportions of TEC even in the same murine cohort.

Given the difficulty of TEC purification, many studies have relied on immunohistochemical techniques that are potentially subjective in their interpretation and often inconsistent due to variations in the field examined. Assessment of the roles played by various thymic events, such as involution, thymic injury, and regeneration, have therefore been compromised. These considerations may be especially important for the analysis of TEC after insults such as chemotherapy or radiation as commonly employed in HSCT. With

¹Experimental Transplantation and Immunology Branch, National Cancer Institute, NIH, Bethesda, Maryland, USA; ²Experimental Immunology Branch, National Cancer Institute, NIH, Bethesda, Maryland, USA.

Correspondence: KM Williams (williak@mail.nih.gov)

DOI: 10.1111/j.1752-8062.2009.00128.x

these cytotoxic therapies, the total thymus anlage is decreased, raising the likelihood that immunohistochemical studies may be subject to variations in the size and depth of sections examined. Using this technique, while studies concur that thymocytes are more radiosensitive than TEC,^{37–39} assessments of TEC alterations after radiation have differed. Some have suggested that the major effects may occur in the medulla with selective depletion of UEA+ medullary TEC^{40,41} and medullary dendritic cells.⁴² In contrast, others have published that the prominent difference after irradiation involves subcortical cells with either an upregulation of K5+K8+ cortical TEC⁴³ or increase in subcapsular cells,³⁷ or a collapse of cortex without alteration in cortical TEC numbers.³⁹ Additionally, although vascular elements have been reported to appear more prominent, most studies agree that, at 1 week postirradiation, this is likely to be an artifact of the test without a true difference in blood vessels between groups.^{37,39} The disparate assessments of TEC changes postirradiation are largely due to inconsistencies in the preparative technique, indicating that a new technique for stromal evaluation is needed.

To best quantify the alterations in TEC, vascular, and dendritic cell subsets after cytotoxic injuries, TEC should be efficiently isolated into single cell suspension with a reproducible technique for subsequent identification. Here, we propose a new method of TEC isolation and evaluate the product of this method by flow cytometry analysis and laser scanning cytometry. We show that this rapid method effectively isolates TEC, endothelial cells, and dendritic cells and yields consistent cell numbers and proportions. We then demonstrate that this method is sensitive enough to detect changes in subsets and total cell number following nonmyeloablative irradiation. These data reveal significant depletion of UEA+ medullary TEC, dendritic cells, and cortical TEC, with an enrichment of fibroblasts following irradiation injury.

Materials and Methods

Animals

Age-matched C57BL/6(B6) female mice were purchased from the Animal Production Unit, National Cancer Institute. Animal care and experimental procedures were carried out under NCI-approved protocols.

New thymic epithelial cell preparation

Thymi from three 4- to 6-week-old female mice were prepared using new TEC preparation method. The thymi were gently separated using forceps. Thymocytes were removed by applying pressure with the head of a syringe to the thymi and washing the remnants three times with RPMI (Invitrogen, Carlsbad, CA, USA). Thymocytes were collected through a 40- μ m mesh. The thymic remnants and any cells caught in the thymocyte mesh were placed in a 20-mL gentleMACS “C” tube (Miltenyi Biotec, Bergisch Gladbach, Germany). Thymic remnants were resuspended in 10 mL of digestion cocktail (0.03 g Liberase Blendzyme 4, Roche Diagnostics, Indianapolis, IN, USA) reconstituted in RPMI and 624 mg DNaseI (tissue culture grade, reconstituted with magnesium). The samples were mechanically disrupted using the Spleen 02 setting on the gentleMACS dissociator, followed by 15-minute digestion at 37°C in the above enzyme cocktail with continuous rotation. Following digestion, the samples were again disrupted using the Spleen 01 setting on the gentleMACS dissociator. The reaction was halted with albumin-rich buffer (500 mL phosphate buffered saline, 0.5% bovine serum albumin, and 2 mM ethylenediaminetetraacetic acid).

The tubes were spun for 7 minutes at 1200 rpm, the supernatant discarded, and the pellet reconstituted with 5 mL of the albumin-rich buffer. At this point, a single cell suspension was evident and the cells were passed over a 40- μ m filter and counted.

Flow cytometry

Single cell suspensions of enriched purified stromal populations and thymocytes were evaluated by flow cytometry. All flow cytometry specimens were incubated with 2.4G2 blocking antibody (anti-mouse CD16/CD32) prior to staining. Samples were labeled using combinations of the following antibodies: CD4 (RM4–5), CD8 (Caltag), UEA (Vector), Ly-51 (BP-1), CD45 biotin (30-F11), CD45 Pacific Blue (30-F11, Invitrogen), MHC class II (25–9–17), EpCAM (Biolegend G8.8). Biotinylated antibodies were developed with streptavidin Pacific Blue (Invitrogen) or PeCy7 (for EpCAM). All antibodies were purchased from BD Biosciences unless indicated otherwise. Isotype controls were utilized for all rare populations, included in full minus one controls. Propidium iodide was used in conjunction with CD45 biotin (developed with streptavidin Pacific Blue) to identify live stromal cells. Panels were acquired on an LSR II flow cytometer (BD Biosciences). All data were analyzed using FlowJo software (Treestar Software). The MHC class II in Allophycocyanin (APC) demonstrated broad range of staining intensity; however, this was not problematic since none of the other fluorochromes required compensation.

Immunofluorescent staining and analysis of tissue sections

Single cell suspensions of enriched purified stromal populations and thymocytes were evaluated by immunohistocytometry. Cells were incubated with 2.4G2 blocking antibody prior to staining. Samples were labeled using combinations of the following antibodies: CD4 (RM4–5), CD8 (Caltag), UEA (Vector), Ly-51 (BP-1), CD45 biotin (30-F11), MHC class II (25–9–17). Biotinylated antibodies were developed with APC-conjugated streptavidin. All antibodies were purchased from BD Biosciences unless indicated otherwise. Hoechst DNA dye (Cambrex Bio Science, Walkersville, MD, USA) was used for visualization of cells. Analysis was done using an iCys laser scanning cytometer (Compucyte Corporation, Westwood, MA, USA) equipped with 488, 594, and 405-nm lasers (for excitation of FITC, Texas red, and Hoechst 33342, respectively). Cells were scanned in 746 \times 100 μ m sections at a 0.5- μ m resolution.

Quantitative reverse transcriptase-PCR

TECs were spun down for 5 minutes at 1,000g and resuspended in RNeasy lysis buffer (Qiagen). Total RNA was prepared using an RNeasy mini RNA isolation kit (Qiagen). cDNA was prepared using the Superscript[®] III RT kit (Invitrogen). Quantitative polymerase chain reaction (PCR) was performed on the Light Cycler 480 using the monocolor hydrolysis probe protocol (Roche).

Statistical analysis

Statistical analysis was performed using Statview 5.0.1 software. All studies were analyzed using unpaired Student's *t*-test.

Results

New rapid separation TEC preparation generates healthy subpopulations

We first investigated whether the new TEC preparation could adequately provide live TEC for flow cytometry evaluation.

Following the new TEC digestion technique, TEC could be consistently identified using flow cytometry (Figure 1A–C). Furthermore, individual live cells (TEC, thymocytes, dendritic cells) could be visualized by immunohistochemistry (Figure 1D–F). Based on propidium iodide discrimination of dead cells, greater than 95% of the total cells in the TEC fraction and greater than 70% of the CD45 negative fraction were viable after preparation with this technique (Figure 1G). All TEC extractions were accomplished in 30 minutes from thymic anlage to TEC single cell suspension. Compared with published TEC preparations,³¹ the new method yielded more easily discernable TEC populations and greater TEC viability. Although the total cell viability exceeded 95% in both methods, the proportion of live cells in the CD45 negative fraction from the previously published method was less than 50% compared to greater than 70% from all experiments with the new method. The new method also improved TEC separation and led to increased recovery of TEC populations, defined by the expression of EPCAM and MHC II, with UEA or Ly51 positivity (Figure 1H).

New technique consistently isolates TEC, endothelial cells, and dendritic cells

Having demonstrated that this technique preserves cell viability and protein expression necessary for flow cytometry analysis, we next evaluated the consistency of this method.

Comparing six groups (18 mice) across different days and with different technicians yielded very similar total proportions and total number of TEC (Figure 2A and B). Finally, dendritic (CD45+ CD11c+) and endothelial cells (CD45– CD31+) were also captured consistently (Figure 2C and D).

New digestion method reveals alterations in thymocyte and TEC populations following irradiation

Having observed that this method of TEC preparation yielded consistent numbers of live cells, we next utilized this method to determine if we could identify changes in TEC following irradiation therapy in a murine model. In order to identify the optimal dose for these experiments, we first determined the effects of increasing radiation doses on thymic size. A linear decrease in thymus weight was observed following escalating radiation doses (Figure 3). A dose of 750 cGy resulted in a significant but moderate decrease in thymus size and was thus chosen to test if our new method could identify radiation-induced changes in TEC populations. We then utilized the new TEC preparation method to evaluate the effect of radiation on TEC and thymocytes. One week after irradiation, the thymic weights and thymocyte number were significantly decreased (Figure 4A). The proportions of thymocytes were also altered after radiation, with a significant depletion of CD4+ and CD4+ CD8+ thymocytes and relative enrichment of CD4– CD8– cells (Figure 4B). Similarly, the stromal populations were differentially affected by radiation. There was a total cell loss of medullary UEA+ TEC, cortical Ly51+ MHC class II+ TEC, and CD45– UEA– Ly51– cells (Figure 4C and D). Radiation selectively decreased the proportion of UEA+ TEC (especially the MHC II high fraction) and MHC class II+ Ly51+ TEC (Figure 4E and F). In contrast, the proportion of Ly51+ cells was increased due to enrichment of fibroblast cells (Ly51+ MHC class II–) (Figure 4E). Decrease in TEC number following irradiation was confirmed by a decrease in total EpCAM gene expression in the digested samples determined by quantitative RT-PCR (Figure 4G). Similar to TEC, dendritic cells were also

significantly depleted following irradiation, while endothelial cells were unaffected (Figure 4H).

Discussion

Emerging clinical data suggest that thymic renewal following stem cell transplantation is critical for optimal immune reconstitution and immunotherapy. Multiple studies have shown that TECs play a critical role in the process of thymic renewal by demonstrating the role of these cells in limiting the thymic niche size, production of factors that fuel thymopoiesis, and mediate central tolerance. The thymic dysfunction that often ensues following stem cell transplantation has been attributed, in part, to the effects of the preparative regimen on TEC. To date, the evaluation of this hypothesis has been hindered by the available techniques for TEC isolation.

To reduce the inconsistencies found in the most commonly used TEC preparation technique, we developed a new method of TEC isolation that incorporated successful elements from the technique originally described Gray et al.^{30,31} The main impetus for this new method was to obviate the need for multiple digestions that might alter viability, proportions, or cell number. Using a new machine that enables mechanical disruption of TEC, we developed a technique that minimized the amount of time required for digestion. Furthermore, incorporating continuous rotation of the sample during digestion also enhanced the separation during a single enzymatic step. We first generated data that showed that this new technique yielded consistent, viable cell numbers of endothelial, epithelial, and dendritic cell, even when performed by multiple investigators at multiple times. Importantly, cell viability was enhanced in the stromal populations of interest. Because the Liberase 4 enzyme can cleave the CD11c epitope used to identify the dendritic cell population, it is possible that dendritic cell numbers are underrepresented, although the proportion of dendritic cells was equivalent to that revealed by the collagenase/dispase method (data not shown). Given that MHC class II staining was not incorporated into the analysis, the proportion of dendritic cells may also be slightly overrepresented as approximately 15% of CD45+ CD11c+ cells (with the new method) lack MHC class II, a requirement for dendritic cell identification.

Having generated data showing that this new TEC isolation method was consistent, we next hypothesized that we could sensitively detect changes in thymocytes and thymic stroma following nonmyeloablative irradiation. Prior studies had suggested that the thymocytes were more susceptible to cell death from radiation than the stroma^{37,38} using immunohistochemical techniques. We show that thymocyte number is more significantly affected than TEC after irradiation by enumeration of cell number of both populations in the same cohort of mice. Studies had also suggested that medullary epithelia and dendritic cells were decreased.^{40–42} Our data corroborated this work and provided further insight. First, we demonstrated a decline in both total cell number and proportion of UEA+ medullary cells. Next, we evaluated the cortical TEC compartment and demonstrated a significant increase in fibroblast number (CD45– LY51+ MHC II–) and concomitant decrease in LY51+ cortical TEC by incorporating MHC class II expression into the phenotype analysis. Finally, we also demonstrated that endothelial cell number did not change with this dose of radiation, consistent with suggestions from prior studies showing a prominence of vasculature due to thymocyte loss rather than changes in endothelial populations.³⁹

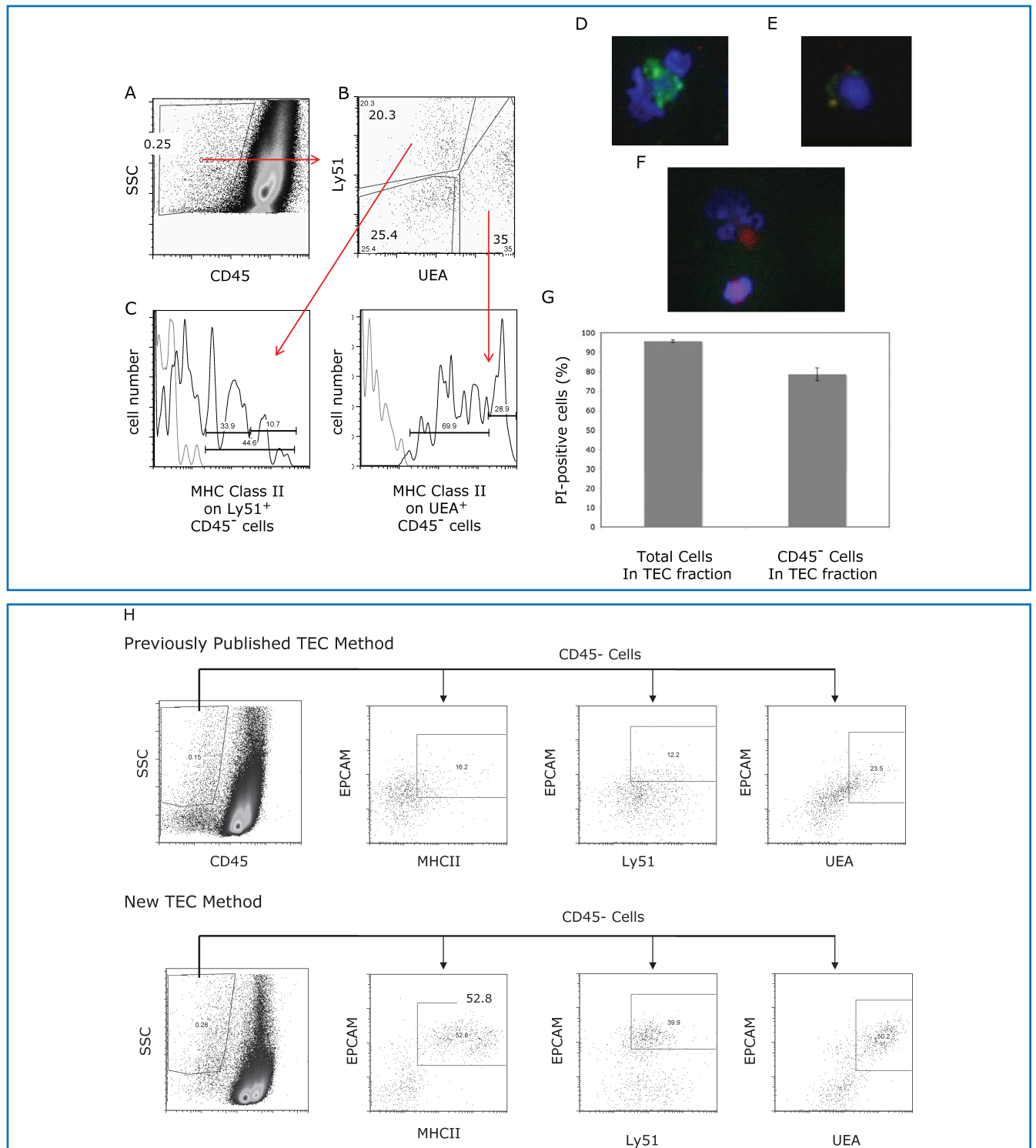


Figure 1. TEC subset identification by flow cytometry and immunohistochemistry. TEC populations were enumerated by flow cytometry, with medullary TEC defined as CD45⁻ UEA⁺, cortical TEC as CD45⁻ Ly51⁺ MHC class II⁺ and a triple-negative population of CD45⁻ UEA⁻ Ly51⁻. Representative flow cytometry plots are shown for **(A)** gating of CD45 negative population and **(B)** discrimination of medullary UEA⁺ TEC and Ly51⁺ populations (cortical TEC and fibroblasts) within the CD45⁻ population, and finally **(C)** MHC class II staining on CD45⁻ Ly51⁺ to discriminate cortical TEC from fibroblasts and CD45⁻ UEA⁺ cells (MHC class II high-proliferating population from the MHC class II intermediate population). For the MHC class II flow cytometry plot, the isotype control is light gray; MHC class II-specific staining is black. TEC populations were directly visualized using immunohistochemical analysis of TEC preparation samples with or without CD45 column depletion. Hoechst DNA dye was utilized to identify live cells. Representative images demonstrate easily discernable single cell suspension of medullary TEC absent CD45 (red) with large nuclei (blue) UEA⁺ (green FITC) **(D)**, likely cortical TEC absent CD45 (red) with Ly51⁺ (PE yellow) and large nuclei (blue) **(E)**, and a thymocyte expressing CD45 (red) with small nuclei (blue) in the lower aspect of the picture with likely dendritic cell (CD45 red positive with large nuclei) in the upper portion of the picture **(F)**. By flow cytometry, viability of the total cell population and the CD45 negative fraction within the TEC fraction using propidium iodide to discriminate dead cells is shown (graph represents four separate TEC preparations of age-matched mice) **(G)**. Representative flow cytometry plots are shown for comparison of the previously published TEC preparation method and the new method **(H)**. The dot plot to the left demonstrates side scatter versus CD45; subsequent plots reveal populations within the CD45 negative fraction, showing MHC class II versus EpcAM and EpcAM⁺ Ly51⁺ (cortical) or UEA⁺ (medullary) TEC.

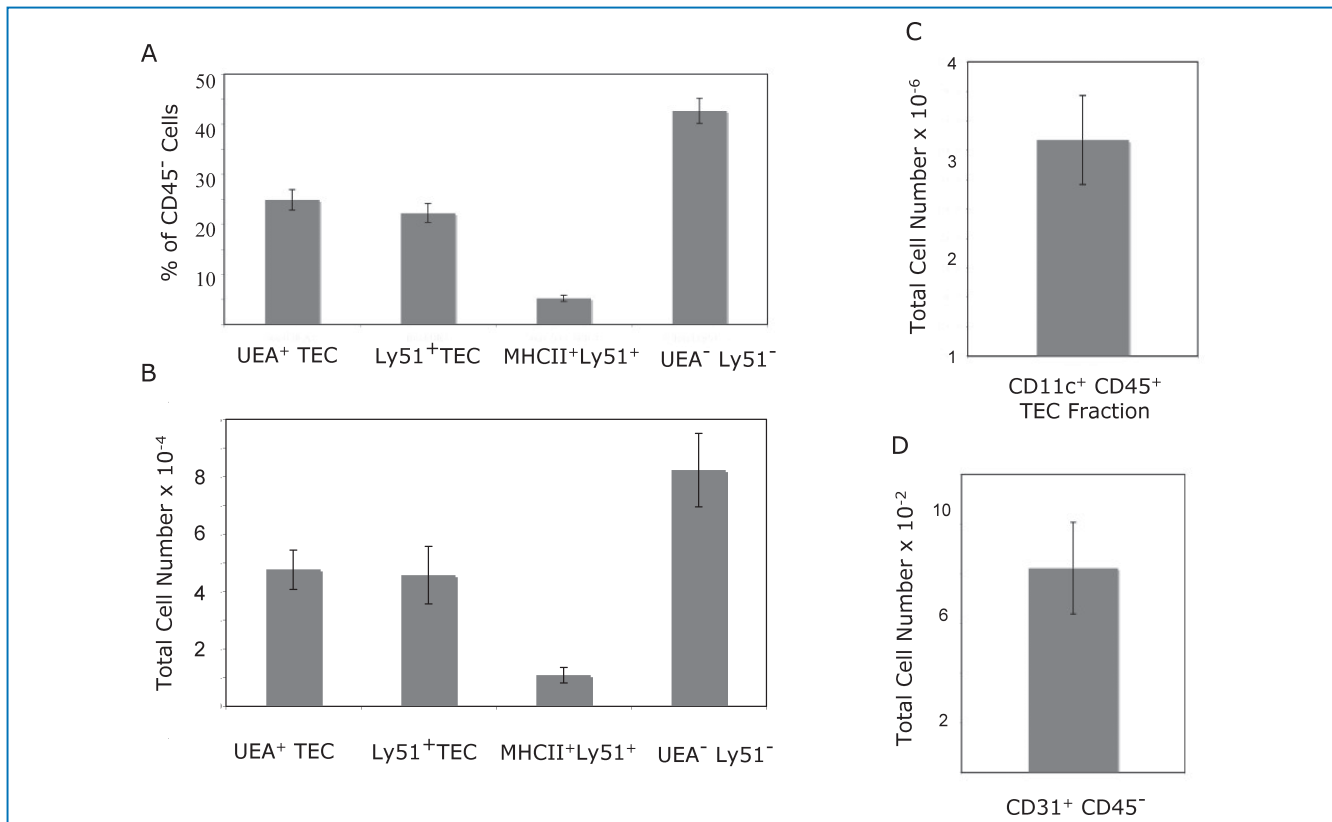


Figure 2. The new method for TEC isolation is reproducible and consistent. Six groups of three age-matched thymi (18 total) were subjected to the new method for TEC isolation using greater than two technicians over multiple days. TEC, dendritic cells, endothelial cells, fibroblasts, and thymocytes were enumerated by flow cytometry after separation using the new method. The proportions of each population within the CD45 negative fraction (A) and total numbers (B) were consistent across experiments and technicians. The dendritic cell (C) and endothelial cell (D) numbers were also reliable across experiments and examiners (standard error bars shown for each population).

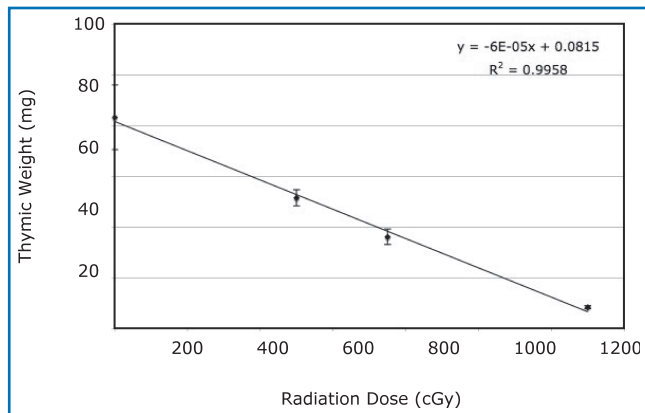


Figure 3. Irradiation linearly decreases thymic size. Six groups of thymi (five per group) received a single dose of radiation and were sacrificed 1 week later without stem cell rescue. The thymic weights were decreased with escalating radiation dose in a linear fashion (standard error bars shown).

These studies may have significant clinical ramifications. Data suggest that UEA⁺ medullary cells contain the highest concentration of the autoimmune regulator gene-expressing cells, a gene critical for the genesis of central tolerance.⁴⁴ Furthermore, these medullary TECs have been previously implicated in thymic regeneration after androgen withdrawal and IGF-1 administration.^{12,14} Thus, the significant loss of medullary TEC may compromise thymic selection, tolerance, and even the ability for thymic renewal. Furthermore, our studies suggest that not

only the thymic cortex collapses after irradiation as shown by Randle-Barrett et al.,³⁹ but also this collapse is accompanied by significant cortical cell loss in total number and proportion. Cortical TECs provide important signals and factors for early thymocyte development. The increase in fibroblasts likely confers a long-term decrease in thymic function through the generation of scar tissue. Kelly et al. have shown that thymic renewal following lethal radiation is enhanced by TEC recovery by showing improved thymic function after lethal radiation with a combination of agents that induced TEC proliferation: androgen withdrawal and keratinocyte growth factor.⁴⁵ Thus, our data and previous data from others suggest that TEC function may underlie the capacity for thymic renewal following stem cell transplantation. Furthermore, in addition to the opportunities for thymic expansion using agents that promote proliferation of TEC, thymopoiesis may also be preserved through TEC-sparing preparative regimens. Studies are underway using this new technique to determine which agents maintain the survival and proliferative capacity of TEC, to design the optimal thymic-sparing bone marrow transplant preparative regimen.

Conclusion

In summary, these data suggest that this effective, consistent, and rapid method of TEC isolation can detect subtle changes in thymic stromal population that demonstrate a depletion in medullary and cortical TEC, dendritic cells, and an enrichment of fibroblasts—all of which may play a significant role in the thymic dysfunction observed following stem cell transplantation.

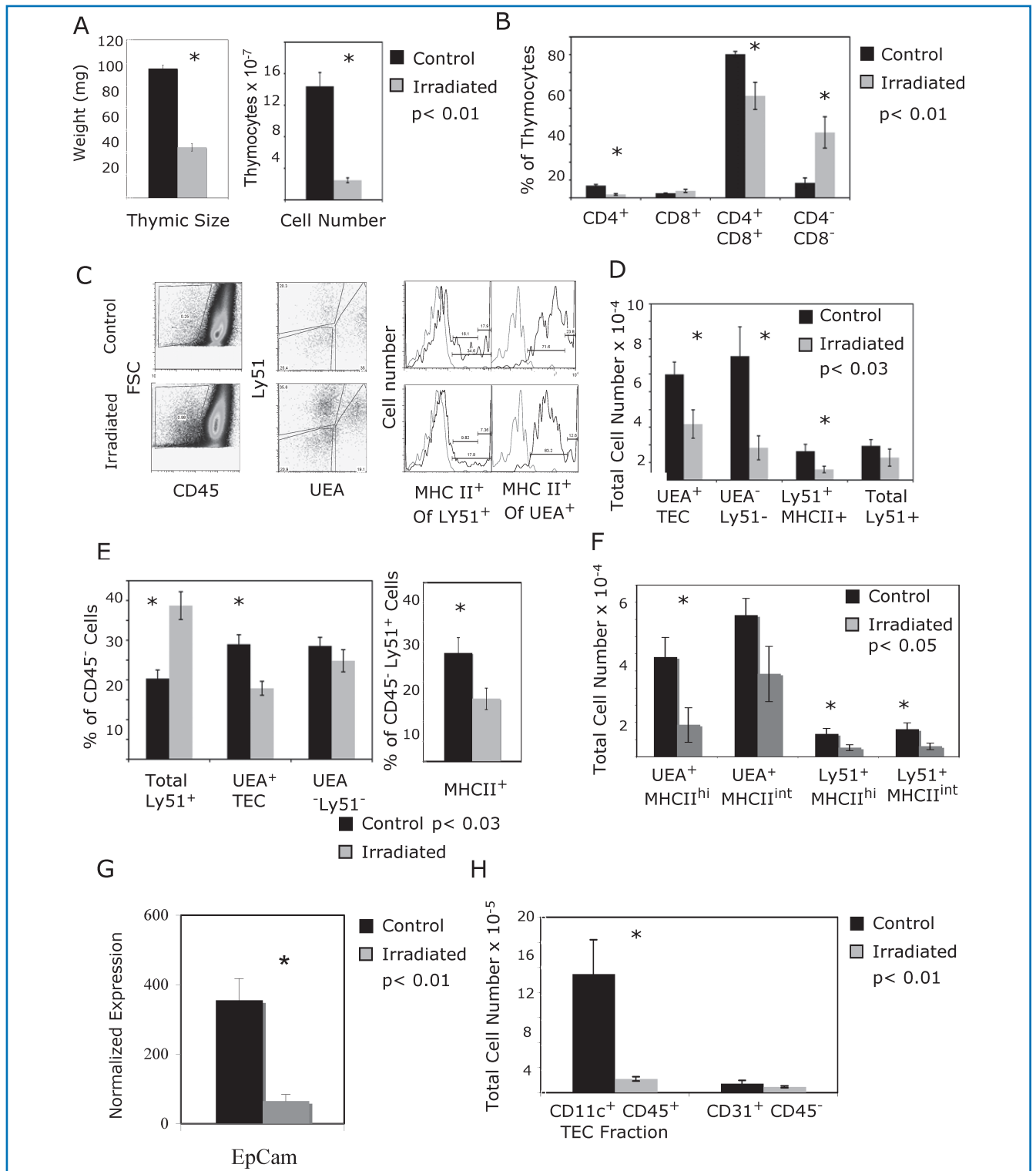


Figure 4. Irradiation selectively decreases cortical and medullary TEC and dendritic cells while sparing fibroblasts and endothelial cells. Six groups of three mice each (18 total) were sacrificed 1 week after receiving 750-cGy irradiation. Using the new isolation method, the separated products (TEC-enriched and thymocytes) were analyzed using flow cytometry. Data represent six experiments with standard error bars. **(A)** Thymic weight and thymocyte number were significantly decreased after irradiation ($p < 0.01$). **(B)** The proportion of single-positive CD4⁺ and CD4⁺ CD8⁺ double-positive thymocytes were significantly decreased following radiation, while the double-negative cells were enriched ($p < 0.01$). The proportion of TEC increases following irradiation **(C)**; however, the total number of TEC is decreased **(D)**. Representative dot plots demonstrate a smaller percentage of TEC in the control mice with greater proportion of UEA⁺ TEC and MHC class II staining on the Ly51 positive cells **(C)**. In contrast, the proportion of Ly51⁺ MHC class II negative cells is greater in the irradiated cohort. This is demonstrated graphically **(E)**. Because published data have suggested that MHC class II high UEA⁺ cells proliferate to the greatest extent,⁴⁶ TECs were individually analyzed with regard to MHC class II expression to identify changes in these subpopulations **(F)**. The greatest cell loss was in the UEA⁺ MHCII high population (3-fold depletion), although cortical TEC populations were also significantly decreased. For the MHC class II flow cytometry plot, the isotype control is light gray; MHC class II-specific staining is black. Loss of TEC number following irradiation was confirmed by RT-PCR of EpCAM gene expression in digested samples **(G)**. EpCAM was normalized to GAPDH; total CD45 negative numbers were then used to normalize to stromal fractions. Finally, the dendritic cell number is significantly decreased following irradiation, while the endothelial cell number is unaffected **(H)**.

Acknowledgments

This study was supported by intramural funds provided by the National Cancer Institute, National Institutes of Health. We thank Yu-Waye Chu for his review of this article. The authors have no conflicting financial interests.

K.M.W., H.M., P.J.L., and W.T. performed research. W.T. and K.M.W. analyzed the data. J.W., K.M.W., and R.E.G. designed research, wrote and edited the paper.

References

- Hakim FT, Memon SA, Cepeda R, Jones EC, Chow CK, Kasten-Sportes C, Odom J, Vance BA, Christensen BL, Mackall CL, Gress RE. Age-dependent incidence, time course, and consequences of thymic renewal in adults. *J Clin Invest*. 2005; 115(4): 930–939.
- Lewin SR, Heller G, Zhang L, Rodrigues E, Skulsky E, van den Brink MR, Small TN, Kernan NA, O'Reilly RJ, Ho DD, Young JW. Direct evidence for new T-cell generation by patients after either T-cell-depleted or unmodified allogeneic hematopoietic stem cell transplantations. *Blood*. 2002; 100(6): 2235–2242.
- Williams KM, Hakim FT, Gress RE. T cell immune reconstitution following lymphodepletion. *Semin Immunol*. 2007; 19(5): 318–330.
- Parkman R, Cohen G, Carter SL, Weinberg KJ, Masinsin B, Guinan E, Kurtzberg J, Wagner JE, Kernan NA. Successful immune reconstitution decreases leukemic relapse and improves survival in recipients of unrelated cord blood transplantation. *Biol Blood Marrow Transplant*. 2006; 12(9): 919–927.
- King C, Ilic A, Koelsch K, Sarvetnick N. Homeostatic expansion of T cells during immune insufficiency generates autoimmunity. *Cell*. 2004; 117(2): 265–277.
- Nordoy T, Husebekk A, Aaberge IS, Jenum PA, Samdal HH, Flugsrud LB, Kristoffersen AC, Holte H, Kvaloy S, Kolstad A. Humoral immunity to viral and bacterial antigens in lymphoma patients 4–10 years after high-dose therapy with ABMT. Serological responses to revaccinations according to EBMT guidelines. *Bone Marrow Transplant*. 2001; 28(7): 681–687.
- Small TN, Papadopoulos EB, Boulad F, Black P, Castro-Malaspina H, Childs BH, Collins N, Gillio A, George D, Jakubowski A, Heller G, Fazzari M, Kernan N, MacKinnon S, Szabolcs P, Young JW, O'Reilly RJ. Comparison of immune reconstitution after unrelated and related T-cell-depleted bone marrow transplantation: effect of patient age and donor leukocyte infusions. *Blood*. 1999; 93(2): 467–480.
- Chen X, Hale GA, Barfield R, Benaim E, Leung WH, Knowles J, Horwitz EM, Woodard P, Kasow K, Yusuf U, Behm FG, Hayden RT, Shurtleff SA, Turner V, Srivastava DK, Handgretinger R. Rapid immune reconstitution after a reduced-intensity conditioning regimen and a CD3-depleted haploidentical stem cell graft for paediatric refractory haematological malignancies. *Br J Haematol*. 2006; 135(4): 524–532.
- Jimenez M, Martinez C, Ercilla G, Carreras E, Urbano-Ispizua A, Aymerich M, Villamor N, Amezcaga N, Rovira M, Fernandez-Aviles F, Gaya A, Martino R, Sierra J, Montserrat E. Reduced-intensity conditioning regimen preserves thymic function in the early period after hematopoietic stem cell transplantation. *Exp Hematol*. 2005; 33(10): 1240–1248.
- Chao NJ, Liu CX, Rooney B, Chen BJ, Long GD, Vredenburgh JJ, Morris A, Gasparetto C, Rizzieri DA. Nonmyeloablative regimen preserves "niches" allowing for peripheral expansion of donor T-cells. *Biol Blood Marrow Transplant*. 2002; 8(5): 249–256.
- Friedman TM, Varadi G, Hopely DD, Filcko J, Wagner J, Ferber A, Martinez J, Brunner J, Grosso D, McGuire L, Kornogol R, Flomenberg N. Nonmyeloablative conditioning allows for more rapid T-cell repertoire reconstitution following allogeneic matched unrelated bone marrow transplantation compared to myeloablative approaches. *Biol Blood Marrow Transplant*. 2001; 7(12): 656–664.
- Williams KM, Lucas PJ, Bare CV, Wang J, Chu YW, Tayler E, Kapoor V, Gress RE. CCL25 increases thymopoiesis following androgen withdrawal. *Blood*. 2008; 112(8): 3255–3263.
- Gray DH, Seach N, Ueno T, Milton MK, Liston A, Lew AM, Goodnow CC, Boyd RL. Developmental kinetics, turnover, and stimulatory capacity of thymic epithelial cells. *Blood*. 2006; 108(12): 3777–3785.
- Chu YW, Schmitz S, Choudhury B, Telford W, Kapoor V, Garfield S, Howe D, Gress RE. Exogenous insulin-like growth factor 1 enhances thymopoiesis predominantly through thymic epithelial cell expansion. *Blood*. 2008; 112(7): 2836–2846.
- Savino W, Postel-Vinay MC, Smaniotto S, Dardenne M. The thymus gland: a target organ for growth hormone. *Scand J Immunol*. 2002; 55(5): 442–452.
- Rossi SW, Jeker LT, Ueno T, Kuse S, Keller MP, Zuklys S, Gudkov AV, Tkahama Y, Krenger W, Blazar BR, Hollander GA. Keratinocyte growth factor (KGF) enhances postnatal T-cell development via enhancements in proliferation and function of thymic epithelial cells. *Blood*. 2007; 109: 3803–3811.
- Alpdogan O, Hubbard VM, Smith OM, Patel N, Lu S, Goldberg GL, Gray DH, Feinman J, Kochman AA, Eng JM, Suh D, Murigan SJ, Boyd RL, van den Brink MR. Keratinocyte growth factor (KGF) is required for postnatal thymic regeneration. *Blood*. 2006; 107(6): 2453–2460.
- Plotkin J, Prockop SE, Lepique A, Petrie HT. Critical role for CXCR4 signaling in progenitor localization and T cell differentiation in the postnatal thymus. *J Immunol*. 2003; 171(9): 4521–4527.
- Hernandez-Lopez C, Varas A, Sacedon R, Jimenez E, Munoz JJ, Zapata AG, Vicente A. Stromal cell-derived factor 1/CXCR4 signaling is critical for early human T-cell development. *Blood*. 2002; 99(2): 546–554.
- Adachi Y, Tokuda N, Sawada T, Fukumoto T. Semiquantitative detection of cytokine messages in X-irradiated and regenerating rat thymus. *Radiat Res*. 2005; 163(4): 400–407.
- Uehara S, Grinberg A, Farber JM, Love PE. A role for CCR9 in T lymphocyte development and migration. *J Immunol*. 2002; 168(6): 2811–2819.
- Wurbel MA, Philippe JM, Nguyen C, Victorero G, Freeman T, Wooding P, Miazek A, Mattei MG, Malissen M, Jordan BR, Malissen B, Carrier A, Naquet P. The chemokine TECK is expressed by thymic and intestinal epithelial cells and attracts double- and single-positive thymocytes expressing the TECK receptor CCR9. *Eur J Immunol*. 2000; 30(1): 262–271.
- Kurobe H, Liu C, Ueno T, Saito F, Ohigashi I, Seach N, Arakaki R, Hayashi Y, Kitagawa T, Lipp M, Boyd RL, Takahama Y. CCR7-dependent cortex-to-medulla migration of positively selected thymocytes is essential for establishing central tolerance. *Immunity*. 2006; 24(2): 165–177.
- Liu C, Saito F, Liu Z, Lei Y, Uehara S, Love P, Lipp M, Kondo S, Manley N, Takahama Y. Coordination between CCR7- and CCR9-mediated chemokine signals in prevascular fetal thymus colonization. *Blood*. 2006; 108(8): 2531–2539.
- Schwarz BA, Sambandam A, Maillard I, Harman BC, Love PE, Bhandoola A. Selective thymus settling regulated by cytokine and chemokine receptors. *J Immunol*. 2007; 178(4): 2008–2017.
- Peschon JJ, Morrissey PJ, Grabstein KH, Ramsdell FJ, Maraskovsky E, Gliniak BC, Park LS, Ziegler SF, Williams DE, Ware CB, Meyer JD, Davison BL. Early lymphocyte expansion is severely impaired in interleukin 7 receptor-deficient mice. *J Exp Med*. 1994; 180(5): 1955–1960.
- Phillips JA, Bronstetter TI, English CA, Lee HE, Virts EL, Thoman ML. IL-7 gene therapy in aging restores early thymopoiesis without reversing involution. *J Immunol*. 2004; 173(8): 4867–4874.
- Prockop SE, Petrie HT. Regulation of thymus size by competition for stromal niches among early T cell progenitors. *J Immunol*. 2004; 173(3): 1604–1611.
- Prockop S, Petrie HT. Cell migration and the anatomic control of thymocyte precursor differentiation. *Semin Immunol*. 2000; 12(5): 435–444.
- Gray DH, Fletcher AL, Hammett M, Seach N, Ueno T, Young LF, Barbuto J, Boyd RL, Chidgey AP. Unbiased analysis, enrichment and purification of thymic stromal cells. *J Immunol Methods*. 2008; 329(1–2): 56–66.
- Gray DH, Chidgey AP, Boyd RL. Analysis of thymic stromal cell populations using flow cytometry. *J Immunol Methods*. 2002; 260(1–2): 15–28.
- Chidgey AP, Pircher H, MacDonald HR, Boyd RL. An adult thymic stromal-cell suspension model for in vitro positive selection. *Dev Immunol*. 1998; 6(3–4): 157–170.
- Klein L, Klugmann M, Nave KA, Tuohy VK, Kyewski B. Shaping of the autoreactive T-cell repertoire by a splice variant of self protein expressed in thymic epithelial cells. *Nat Med*. 2000; 6(1): 56–61.
- Mostafaie A, Bidmeshkipour A, Shirvani Z, Mansouri K, Chalabi M. Kiwifruit actinidin: a proper new collagenase for isolation of cells from different tissues. *Appl Biochem Biotechnol*. 2008; 144(2): 123–131.
- Klug H, Mager B. Ultrastructure and function of interdigitating cells in the guinea pig thymus. *Acta Morphol Acad Sci Hung*. 1979; 27(1–2): 11–19.
- Drumea-Mirancea M, Wessels JT, Muller CA, Essl M, Eble JA, Tolosa E, Koch M, Reinhardt DP, Sixt M, Sorokin L, Stierhof YD, Schwarz H, Klein G. Characterization of a conduit system containing laminin-5 in the human thymus: a potential transport system for small molecules. *J Cell Sci*. 2006; 119(Pt 7): 1396–1405.
- Irifune T, Tamechika M, Adachi Y, Tokuda N, Sawada T, Fukumoto T. Morphological and immunohistochemical changes to thymic epithelial cells in the irradiated and recovering rat thymus. *Arch Histol Cytol*. 2004; 67(2): 149–158.
- Arudchelvan Y, Tokuda N, Adachi Y, Sawada T, Fukumoto T. Ultrastructural alterations of the cortical epithelial cells of the irradiated and recovering rat thymus. *Arch Histol Cytol*. 2005; 68(3): 205–212.
- Randle-Barrett ES, Boyd RL. Thymic microenvironment and lymphoid responses to sublethal irradiation. *Dev Immunol*. 1995; 4(2): 101–116.
- Adkins B, Gandour D, Strober S, Weissman I. Total lymphoid irradiation leads to transient depletion of the mouse thymic medulla and persistent abnormalities among medullary stromal cells. *J Immunol*. 1988; 140(10): 3373–3379.
- Wang Y, Tokuda N, Tamechika M, Hashimoto N, Yamauchi M, Kawamura H, Irifune T, Choi M, Awaya A, Sawada T, Fukumoto T. Vascular and stromal changes in irradiated and recovering rat thymus. *Histol Histopathol*. 1999; 14(3): 791–796.
- Beschorner WE, Armas OA. Loss of medullary dendritic cells in the thymus after cyclosporine and irradiation. *Cell Immunol*. 1991; 132(2): 505–514.
- Popa I, Zubkova I, Medvedovic M, Romantseva T, Mostowski H, Boyd R, Zaitseva M. Regeneration of the adult thymus is preceded by the expansion of K5+K8+ epithelial cell progenitors and by increased expression of Trp63, cMyc and Tcf3 transcription factors in the thymic stroma. *Int Immunol*. 2007; 19(11): 1249–1260.
- Anderson MS, Venanzi ES, Klein L, Chen Z, Berzins SP, Turley SJ, von Boehmer H, Bronson R, Dierich A, Benoist C, Mathis D. Projection of an immunological self shadow within the thymus by the aire protein. *Science*. 2002; 298(5597): 1395–1401.
- Kelly RM, Highfill SL, Panoskaltsis-Mortari A, Taylor PA, Boyd RL, Hollander GA, Blazar BR. Keratinocyte growth factor and androgen blockade work in concert to protect against conditioning regimen-induced thymic epithelial damage and enhance T-cell reconstitution after murine bone marrow transplantation. *Blood*. 2008; 111(12): 5734–5744.
- Gray D, Abramson J, Benoist C, Mathis D. Proliferative arrest and rapid turnover of thymic epithelial cells expressing Aire. *J Exp Med*. 2007; 204(11): 2521–2528.